Local Structural and Tracer Diffusion Mechanism in Amorphous Fe-based Alloys

Pham Huu Kien[1*]

[1]*Department of Physics, Thainguyen University of Education, Luong Ngoc Quyen Road, Thainguyen, Vietnam.*

Author's contribution

This work was carried out by author PHK. Author designed the study, performed the statistical analysis, wrote the protocol, wrote the first draft of the manuscript, managed literature searches, and managed the analyses of the study and literature searches. Author read and approved the final manuscript.

ABSTRACT

Local structure and tracer diffusion mechanism in amorphous Fe and $Fe_{80}B_{20}$ solids is studied using the statistic relaxation (SR) model containing 2×10^5 atoms. It was found a large number of bubbles which could break-up and leads to diffusion. A bubble diffusion mechanism is proposed and the diffusion coefficient determined in term of this mechanism is in reasonable agreement with experimental data. The decrease in diffusion coefficient upon thermal annealing observed experimentally for most amorphous Fe-based alloys is interpreted as a result of reduced number of bubbles in system.

1. INTRODUCTION

Amorphous Fe-based alloy (AFbA) is a material of much technological relevance and has important implications in material science and geophysics [1-7]. It is found many specific properties of diffusion in AFbA compared to crystal counterpart. For example, the tracer-diffusivity in well-relaxed specimen is much slower than one in as-quenched sample [8-12]. This relaxation effect commonly is interpreted by the reduction of quasi-vacancies in super-

---

*Corresponding author: E-mail: huukienpham@yahoo.com;

saturation until the relaxation is over. In well-relaxed state, conversely, the tracer atoms diffuse via collective movement of a group of neighboring atoms. However, the experimental data in ref. [13,14] are in contradiction to that the diffusion mechanism just described predicted. Simulation, on other hand reveals unstableness of vacancies in amorphous matrix. Several works found a continuous spectrum of spherical voids in AFbA, but their size is less than atomic radius [15-17]. The free volume model is also employed to interpret the diffusion behavior of AFbA, but it cannot properly describe the diffusivity in AFbA such as Fe-Ni-B which show the cooperative activated movement more like diffusivity in solid state than in liquid [13,18,19]. In ref. [20], Sietsma analyzed different types of holes in amorphous alloy and found that the number of holes surrounding by ten or more atoms decreases strongly in well-relaxed sample. Furthermore, he argues the importance of big holes for atomic diffusivity. Previous study shows that the atomic cage like bubble functions as diffusion vehicle for amorphous alloys. The bubble represents a spherical void with five or more atoms lied on its surface [21]. However, the analysis of this study bases only on amorphous $Fe_{80}B_{20}$ alloy. Therefore, a systematic study of all types of bubbles in AFbA has been done in present papers in order to clarify the importance of bubbles for atomic diffusivity in AFbA.

2. CALCULATION METHOD

The simulation has been conducted for the model consisting of 2×10^5 atoms in a cubic box with periodic boundary conditions. We use the Pak-Doyama potential [17] and the density is taken from real AFbA. This potential has following formula

$$\varphi\left(r_{ij}\right) = a\left(r_{ij}+b\right)^4 + c\left(r_{ij}+d\right)^2 + e \qquad r_{ij} \leq r_{cutoff} \tag{1}$$

r_{ij} is the distance between the ith and j^{th} atoms, r_{cutoff} is the minimum position of the first peak in the pair radial distribution functions. The parameters *a*, *b*, *c*, *d*, *e* and r_{cutoff} are given in Table 1. This work we employ SR method [17] which provides the structure of AFbA similar to that the low-temperature structure of real AFbA. Accordingly, each atom moves by a length *dr* in the direction of the force acting on it from all remaining atoms. The length *dr* is equal to 0.02 or 0.4 Å. This movement is repeated many times until the system reaches an equilibrium state. Model was prepared by relaxing with a SR step length of 0.4 Å, this process is like shaking many times the atomic arrangement in model. Then we relax the obtained model with the SR step length 0.02 Å to reaches a new equilibrium.

Table 1. The parameters of the inter-atomic potential (1)

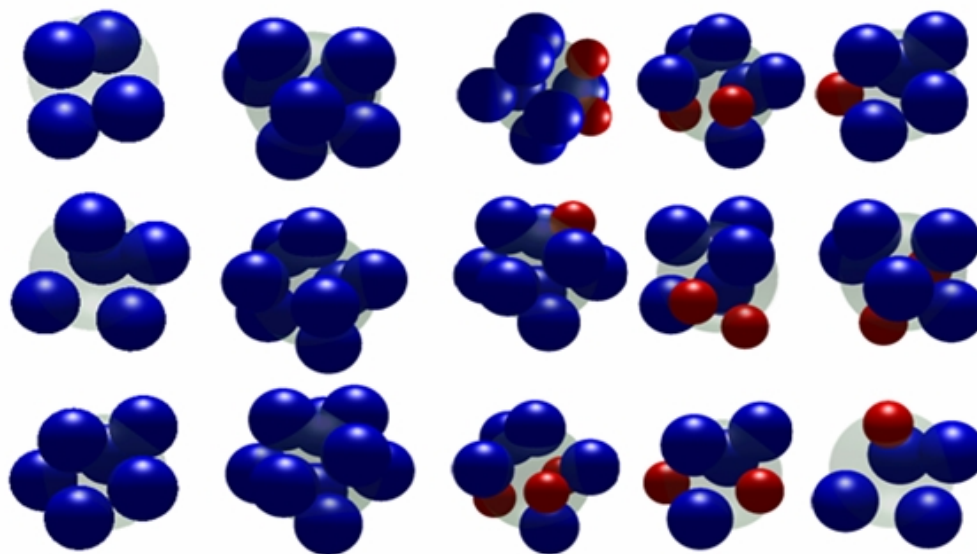| Pairs	*a* (eV/ Å⁴)	*b* (Å)	*c* (eV/ Å²)	*d* (Å)	*e* (eV)	r_{cutoff} (Å)
Fe-Fe	- 0.18892	- 1.82709	1.70192	- 0.50849	- 0.19829	3.44
Fe-B	- 0.22407	- 1.47709	2.01855	- 2.15849	- 0.23519	3.09
B-B	- 0.08772	- 2.17709	0.79028	- 2.85849	- 0.09208	3.79

Fig. 1. The snapshot of typical simplexes detected in the Fe-based alloys. Blue and red spheres indicate iron and boron atoms, respectively

Initial configuration is generated by randomly placing all atoms in a simulation box. Then the model is relaxed over 10^3 steps until the system attains the equilibrium, e.g., the energy of system fluctuates around a constant value and the pressure is equal to zero. The model M_1 (Fe) and M_3 ($Fe_{80}B_{20}$) is constructed by relaxing with dr = 0.4 Å over 200 SR steps and then is treated with dr = 0.02 Å by 10^6 SR steps. To investigate the relaxation effect three additional models (model M_2, M_4 and M_5) are prepared with the same density as the model M_1 or M_3, but their potential energy is lower (Table 2). Lower energy model (model M_2, M_4 and M_5) can be constructed by many times relaxing the model M_1 or M_3 with dr = 0.4 Å and then they are again relaxed with dr = 0.02 Å until the system reaches a new equilibrium. As in the previous work [21], we consider four neighboring atoms forming a tetrahedron and a circum-sphere of this tetrahedron (CS), e.g. CS's surface passes through vertices of the tetrahedron. We consider only the CS not containing any atom inside. Let R_B be the radii of CS and n_B be the number of atoms located from CS center at distance $R_B \pm 0.1$ Å. Hereafter we call it n_B-simplex with radius RB. Several types of n_B-simplex detected in AFbA are shown in Fig. 1. If n_B or R_B is enough large, then n_B-simplex form an atomic cage like a bubbles, e.g. a large group of atoms gathered around a large void. The bubble is unstable and it may break up leading to diffusion. The number of bubbles in models weakly depends on temperature, but very sensitive to the relaxation degree. Therefore, it is interesting to clarify which one among n_B-simplexes is bubble and how bubbles break up.

3. RESULTS AND DISCUSSION

3.1 The Structural

Structural factors (SF) in AFbA have been studied both by the neutron and x-ray diffraction techniques. Our simulation can be compared to these experiments and therefore allowed us to test the reliability of model. As shown in Fig. 2, compared to experimental data in ref.

[22,23] the SF is good agreement with simulation result. For partial radial distribution functions (PRDFs) it is clearly seen the splitting of second peak which is thought to be a typical feature for metalloid-metal alloys (Fig. 3). As shown in Fig. 3 the PRDFs of M_1, M_2 and M_3, M_4, M_5 models are similar form. This result indicates the relaxation degree almost does not affect on PRDFs, but it is reflected by the concentration of simplex which will be shown later.

Table 2. The characteristics of models and n_B-simplexes: Here ε is the mean potential energy per an atom; n_B is the number atoms on simplex; R_B (Å) is the radius of simplex

Models	M_1	M_2	M_3	M_4	M_5
ε (eV)	**-1.384**	**-1.394**	**-1.459**	**-1.489**	**-1.519**
$n_B = 5$	0.24×10^0	0.23×10^0	1.03×10^0	1.00×10^0	0.97×10^0
$n_B = 6$	1.13×10^{-2}	1.08×10^{-2}	1.76×10^{-1}	1.58×10^{-1}	1.51×10^{-1}
$n_B = 7$	8.51×10^{-5}	0	8.23×10^{-3}	8.79×10^{-3}	5.46×10^{-3}
$n_B = 8$	0	0	0.64×10^{-3}	0.67×10^{-3}	0.08×10^{-3}
$n_B = 9$	0	0	0.09×10^{-3}	0.01×10^{-3}	0
$R_B = 1.8$	0.740	0.718	0.298	0.292	0.284
$R_B = 1.9$	0.082	0.064	0.067	0.053	0.04
$R_B = 2.0$	0.032	0.021	0.027	0.021	0.01
$R_B = 2.1$	0.008	0.004	0.009	0.007	0.002
$R_B = 2.2$	0.002	0.001	0.002	0.001	0
$R_B = 2.3$	0.010×10^{-2}	0	0.070×10^{-2}	0.008×10^{-2}	0.001×10^{-2}
$R_B = 2.4$	0.001×10^{-3}	0	0.020×10^{-3}	0.009×10^{-3}	0.002×10^{-3}

Table 2 shows that the number n_B atoms increases the number of corresponding n_B-simplexes significantly decreases. Compared to iron model the amount of 7-, 8- and 9-simplex in $Fe_{80}B_{20}$ model is much bigger. It indicates that the structure of $Fe_{80}B_{20}$ model is more inhomogeneous than iron model. As shown in Table 2, the amount of simplexes strongly decreases with increasing their radius R_B. Furthermore, the number of large simplexes detected in $Fe_{80}B_{20}$ model (R_B bigger than 1.9 Å) is significantly bigger than one for iron model. This evidences the structure of $Fe_{80}B_{20}$ model is more inhomogeneous than iron model.
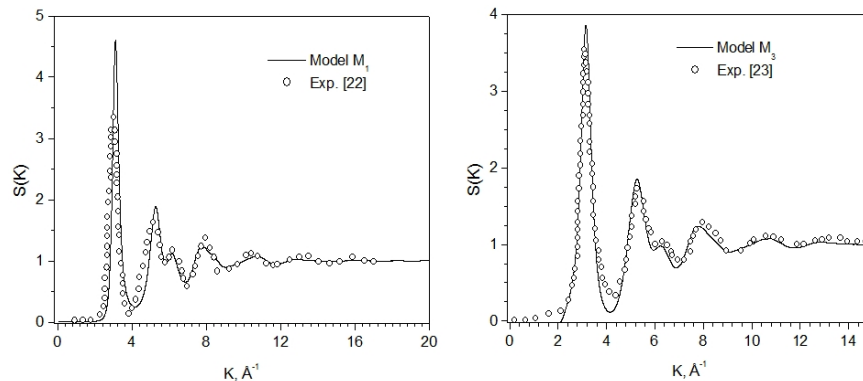

Fig. 2. The structure factor Fe (left) and $Fe_{80}B_{20}$ (right) amorphous models

As mention above the relaxation degree characterized by mean of energy per atom (Table 2) decreases in the following order: M_1, M_2 for iron model and M_3, M_4, M_5 for $Fe_{80}B_{20}$ model. From data in Table 2 it follows that the simplexes with large n_B or radius R_B are annihilated upon relaxation. Note that the shortest distance between two atoms Fe in the structure of considered model is near 1.9 Å. It means that the free volume inside simplex with $R_B > 1.9$ Å is enough large such that one can place one iron atom in it. Therefore, such simplex resembles the crystalline vacancy on base of geometrical consideration.
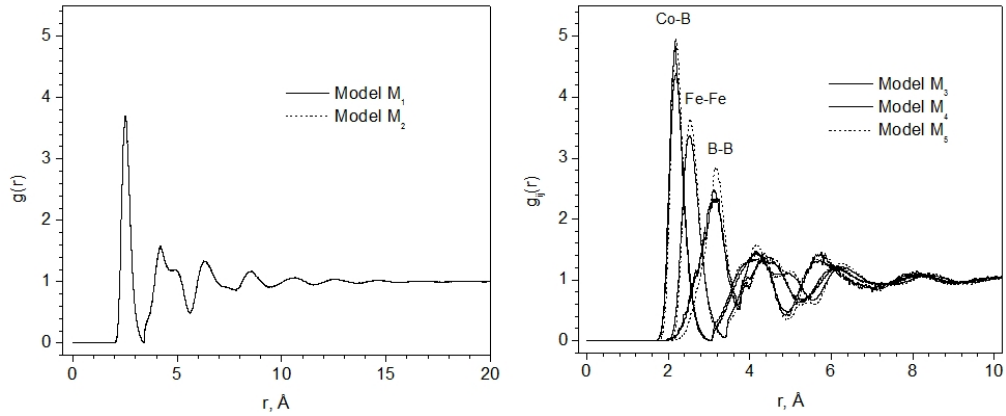

Fig. 3. The partial radial distribution functions Fe (left) and $Fe_{80}B_{20}$ (right) models
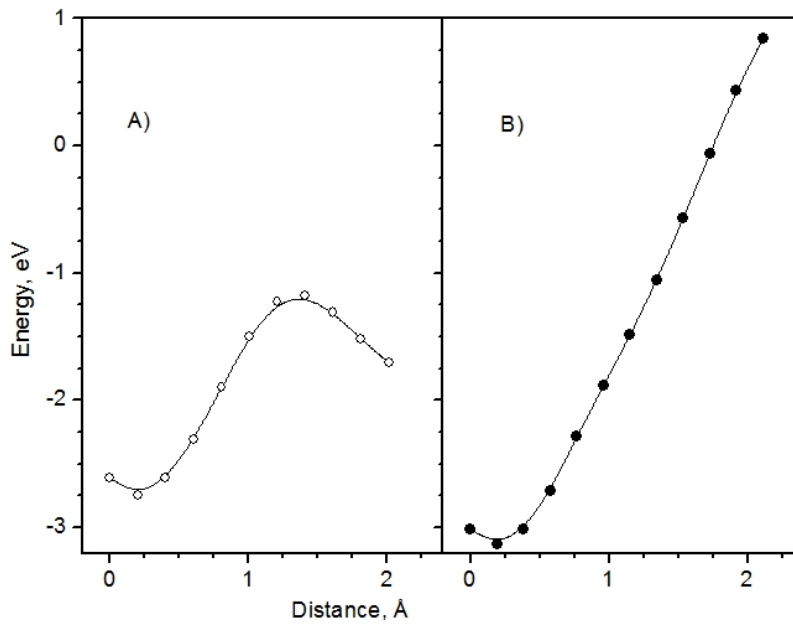
3.2 Bubbles and Diffusion Mechanism

Fig. 4. Potential energy profiles for atom moving into simplex

Table 3. The mean square displacement and number of bubbles in amorphous Fe-based alloys: Here $<x_{Fe}^2>$, $<x_B^2>$, m_{Fe} and m_B are the mean square displacement and number of bubbles of Fe and B atoms, respectively

Models	m_{Fe} (×10^{-4})	m_B (×10^{-4})	Iron		Boron	
			$<x_{Fe}^2>$, Å^2	$<x_B^2>$, Å^2	$<x_{Fe}^2>$, Å^2	$<x_B^2>$, Å^2
M$_1$	0.65	–	7.791	–	–	–
M$_2$	0.31	–	5.817	–	–	–
M$_3$	4.72	7.72	7.140	0.508	0.613	4.092
M$_4$	2.34	6.27	6.482	0.251	0.758	4.478
M$_5$	0.28	3.82	5.664	0.321	0.447	4.171

As shown in ref. [20], big holes which are surrounding by ten or more atoms can break up and lead to tracer diffusion. In our simulation the number n_B is correlated with radius R_B. Hence large simplex has large R_B or large number n_B and simplex is to be regarded like "big hole". In order to clarify how the bubble breaks up, for every simplex we determined the potential energy variation of neighboring atom as it moves step by step on a line connecting their initial position with the simplex center. The potential energy profiles (PEPs) for atom moving into simplex are shown in Fig. 4. There are two types of PEP. First one corresponding to curve B monotonously increases with the distance. The potential barrier in this case is too high such that atom can not do jump. Second one corresponding to curve A has a maximum and the potential barrier lies in the interval from 0.6 to 3.2 eV (Fig. 5). Here, the potential barrier is determined by the difference between the maximum point in the potential energy profile (PEP) and the site energy of the diffusion atom. It means that the jump can be realized and this simplex could break up by the jump of one neighboring atom. This simplex is called a bubble. Based on the analyzing PEPs for all simplexes the number of bubbles is calculated and presented in Table 3. For bubbles the radius R_B and number n_B is found to be larger than 1.9 Å and 6 respectively. There are two types of bubbles which correspond to the type of jumping atom (iron or boron). Furthermore, the number of bubbles also monotonously decreases with relaxation degree. The distribution of potential barrier for bubbles is shown in Fig. 5 and it can be fitted by the expression

$$f\left(\varepsilon_{bar}\right) = A \exp\left[-\left(\frac{\varepsilon_{bar} - \varepsilon_{av}}{\sigma} \right)^2 \right] \tag{2}$$

Where ε_{av} is averaged barrier height, σ is the width of $f(\varepsilon_{av})$, A is normalizing constant. The parameter σ, ε_{av} are equal to 0.46, 1.63 for Fe$_{80}$B$_{20}$ and 0.71, 1.65 eV for Fe model, respectively. As shown in Fig. 5, the distribution of potential barrier is Gauss function both of Fe and Fe-B models. Compared to iron model the distribution of potential barrier in Fe$_{80}$B$_{20}$ is higher and narrower. Fig. 6 shows bubble's distribution in AFbA. It can be seen some clusters of bubbles where several bubbles gather at one place. This place obviously has low local density compared to the mean density of the system. Therefore, the inhomogeneity in AFbA structure is characterized by bubbles and their clusters. The more the system relaxes, the less the concentration of bubbles and bubbles clusters.
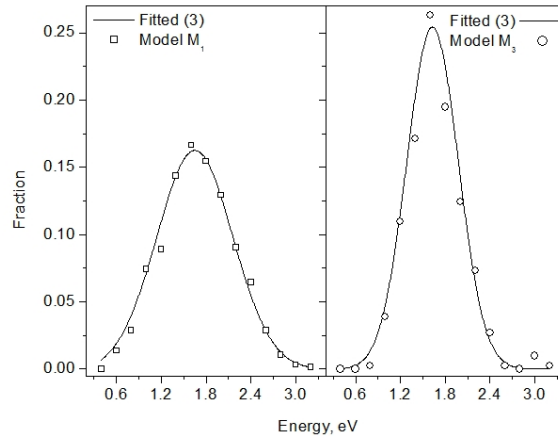
Fig. 5. The distribution forms of potential barriers in Fe-based alloys

Table 4. The diffusion coefficient of amorphous Fe-based alloys at 570-640 K

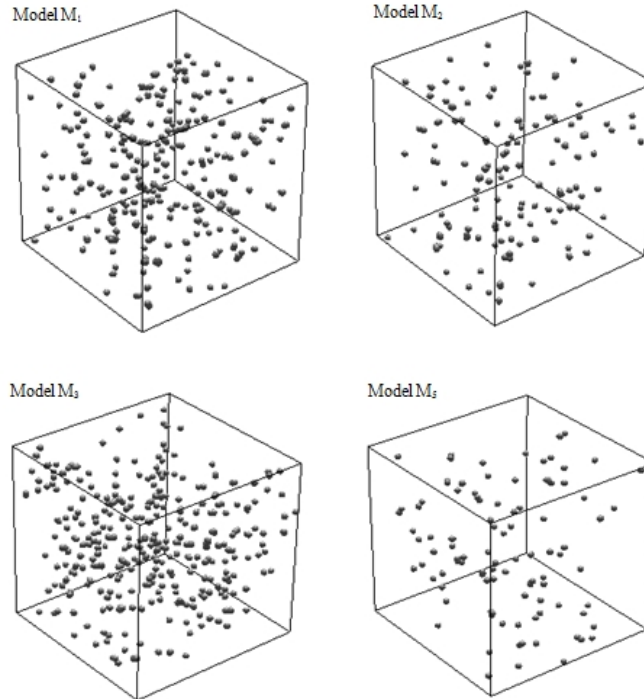| Systems	D_{Fe}, m^{2}s^{-1}	D_B, m^{2}s^{-1}	Reference
Model M$_1$	$1.5 \times 10^{-19} - 2.0 \times 10^{-18}$	$--$	This work
Model M$_3$	$2.6 \times 10^{-22} - 1.2 \times 10^{-21}$	$8.2 \times 10^{-22} - 8.8 \times 10^{-21}$	This work
Fe$_{80}$B$_{20}$	$2.2 \times 10^{-23} - 5.2 \times 10^{-21}$	$--$	[14]
Fe$_{40}$Ni$_{40}$B$_{20}$	$4.7 \times 10^{-23} - 8.8 \times 10^{-21}$	$1.7 \times 10^{-21} - 1.4 \times 10^{-19}$	[2]

Fig. 6. The bubbles's distribution in simulation box; the sphere represents the CST
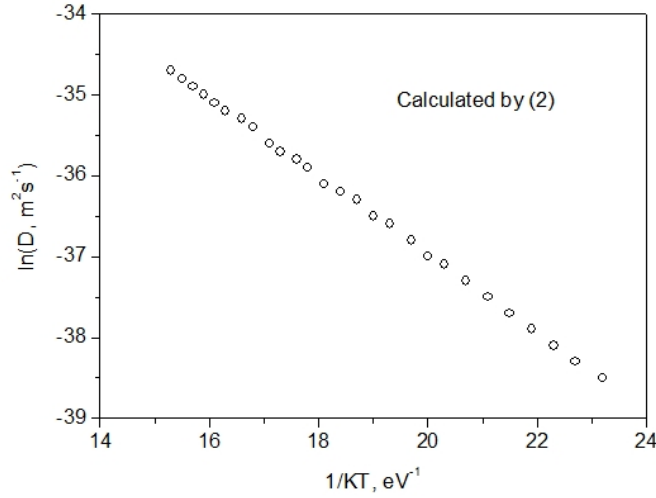
Fig. 7. The temperature dependence follows Arrehenius behavior for model M₁

Important quantity used to estimate the diffusion coefficient is the mean square displacement of atoms upon breaking up the bubbles. To calculate this quantity we select the atom which can realize the jump and move it into the bubbles. Then the system is relaxed until reach the equilibrium. Result is presented in Table 3. The mean square displacement of all atoms is equal to $<x_{Fe}^2> + <x_B^2>$. It is clear that the breaking up bubble leads to collective movement of all atoms located nearby bubble. The value of $<x_{Fe}^2>$ and $<x_B^2>$ for less relaxed sample (model M₁ and M₃) is bigger than ones for more fully relaxed sample (model M₂, M₄ and M₅). After breaking up the bubble it is interesting to examine the total number of bubble in the system. The result shows that unlike the vacancy movement in crystalline lattice the present bubble disappears, but sometime new bubbles are created in the system. Combined these results a tracer diffusion mechanism is proposed as follows: AFbA contains a number of bubbles which weakly depends on temperature, but very sensitive to the relaxation degree. The bubble is enough large such that one can place an atom inside. The breaking up bubble leads to collective movement of atoms located nearby the present bubble. The number of bubbles decreases upon relaxation, but their full annihilation is completed only when the AFbA crystallizes. However, we can turn on to estimate the diffusion coefficient D_S of suggested mechanism by the expression

$$D_S = \mu f \frac{1}{n_{atom}} \upsilon \left[m_{Fe} <x_{Fe}^2>_S + m_B <x_B^2>_S \right] \tag{3}$$

Where S is denoted to Fe or B, μ is the geometrical correlation factor, n_{atom} is the number of atoms in simulation box, f is the correlation factor for consecutive hops. Taking the free energy for atomic jump to consist of the potential barrier ε_{bar} and the migration entropy Δs_m of the jumping frequency becomes

$$\upsilon = \upsilon_0 \int_{\varepsilon_{min}}^{\varepsilon_{max}} \exp\left[-\left(\frac{\varepsilon_{bar} - \varepsilon_{av}}{\sigma} \right)^2 \right] \exp\left(-\frac{\varepsilon_{bar}}{k_B T} \right) \exp\left(\frac{\Delta s_m}{k_B} \right) d\varepsilon_{bar} \tag{4}$$

Where v_o is the attempt frequency ($\sim 10^{12} \text{s}^{-1}$); k_B is the Boltzmann constant and T is the temperature. Assuming $\mu = 1/6$, $\exp(\Delta s_m/k) \approx 1$ and $f = 1$ and using data from Table 3 and equation (3), the diffusion coefficient is calculated and presented in Table 4 and Fig. 7. For the temperature interval of 570-640 K the calculation result is in reasonable agreement with experimental data for AFbA with close chemical composition. The diffusion coefficient based on bubble mechanism is found to obey the Arrehenius law as shown in Fig. 7. Furthermore, from Table 3 and equation (3) show that decreasing the diffusion coefficient related to the reduction of number of bubbles with increasing the relaxation degree.

4. CONCLUSION

We investigated the tracer diffusion in AFbA model using statistic relaxation method. Our simulation shows that the most of models contain a number of large n_B-simplexes which like the bubble in the amorphous matrix. Compared to iron model, $Fe_{80}B_{20}$ model contains much larger amount of large simplexes indicating its more inhomogeneous structure. The bubble is enough large such that one can place one atom inside. Furthermore, they can break up and such lead to diffusion. It is found that the simplex with $n_B > 6$ or $R_B > 1.9$ Å could be bubbles. A diffusion mechanism is suggested that the bubble breaks up by jump of neighboring atom and then collective movement of atoms located nearby occurs. The number of bubbles weakly depends on the temperature, but is sensitive to the relaxation. The result shows that the diffusion coefficient determined in term of the suggested mechanism is good agreement with experiment data and Arrhenius law. The relaxation effect concerning the reduction of diffusion coefficient upon thermal annealing is interpreted as result of annihilation of bubbles.

ACKNOWLEDGEMENTS

COMPETING INTERESTS

Author has declared that no competing interests exist.

REFERENCES

1. Horvath J, Ott J, Pfahler K, Ulfert W. Tracer diffusion in amorphous alloys. Mater. Sci. Eng. 1988;97:409-413.
2. Pavlovsky J, Ulfert W, Frank W. Self-diffusion of ^{58}Co in amorphous $Co_{79}Nb_{14}B_7$ during isothermal crystallization. Mater. Chem. Phys. 1994;36:383-388.
3. Frank W, Horner A, Scharwaechter P, Kronmiiler H. Diffusion mechanisms in amorphous alloys. Mater. Sci. Eng. 1988;97:415-418.
4. Tyagi AK, Macht MP, Naundorf V. Diffusion coefficients of ^{63}Ni in $Fe_{40}Ni_{40}B_{20}$ metallic glass. Acta Metall. Mater. 1991;39:609-617.
5. Ulfert W, Horvath J, Frank W, Kronmfiller H. Self-diffusion of 59Fe tracer atoms in amorphous $Fe_{78}Si_9B_{13}$ and $Fe_{40}Ni_{40}B_{20}$. Cryst. Latt. Def. Amorph. Mater. 1989;18:519-531.
6. Flege S, Fecher U, Hahn H. Diffusion in amorphous NiZrAl alloys. J. Non-Cryst. Solids. 2000;270:123-128.
7. Calm RW, Evetts JE, Patterson J, Somekh RE, Jackson CK. Direct Measurement by SIMS of Self-Diffusion of Boron in $Fe_{40}Ni_{40}B_{20}$ Glass. J. Mater. Sci. 1980;15:702-710.

8. Chakravarty S, et al. Fe and N self-diffusion in amorphous FeN: A SIMS and neutron reflectivity study. Acta Materialia 2009;57:1263-1271.
9. Van den Beukel A, Sietsma J. Flow defects and diffusion defects in metallic glasses. Mater. Sci. Eng. 1991;134(A):935-938.
10. Sharma SK, Banerjee S, Kuldeep, Jain AK. A comparative study of thin film diffusion measurements in metallic glasses by Rutherford backscattering spectrometry and Auger electron spectroscopy. Acta Metall. 1988;36:1683-1690.
11. Roos WD, Plessis JD, van Wyk GN. Diffusion of silicon in Fe-based amorphous and crystalline alloys. Appl. Surf. Sci. 1990;40:303-307.
12. Limoge Y. Role of energetic disorder on diffusion in amorphous alloys. J. Non-Cryst. Solids 1990;117-118:605-608.
13. Ruitenberg G, de Hey P, Sommer F, Sietsma J. Pressure dependence of the free volume in amorphous $Pd_{40}Ni_{40}P_{20}$ and its implications for the diffusion process. Mater. Sci. Eng. 1997;226-228(A):397-400.
14. Limoge Y. Activation volume for diffusion in a metallic glass. Acta Metall. Mater. 1990;38:1733-1742.
15. Averback RS. Defects and diffusion in amorphous alloys. MRS Bulletin. 1991;16:47-52.
16. Limoge Y. Microscopic and macroscopic properties of diffusion in metallic glasses. Mater. Sci. Eng. 1997;226-228(A):228-236.
17. Hung PK, Hue HV, Vinh LT, "Simulation study of pores and pore clusters in amorphous alloys $Co_{100-x}B_x$ and $Fe_{100-y}P_y$. J. Non-Cryst. Solids. 2006;352:3332-3338.
18. Zhu A, Shiflet GJ, Poon SJ. Diffusion in Metallic Glasses - Analysis from the Atomic Bond Defect Perspective. Acta Materialia. 2008;56:3550-3557.
19. Naundorf V, et al. The pre-factor, D_0 of the diffusion coefficient in amorphous alloys and in grain boundaries. J. Non-Cryst. Solids. 1998;224:122-134.
20. Sietsma J and Thijsse BJ. Characterization of free volume in atomic models of metallic glasses. Phys. Rev. B. 1995;52:3248-3255.
21. Hung PK, Kien PH and Vinh LT. Evidence of 'microscopic bubbles' and a new diffusion mechanism for amorphous alloys. J. phys.Condens. Matter. 2010;22:035401,1-5.
22. Waseda Y, Chen HS. A structural study of metallic glasses containing boron (Fe-B, Co-B and Ni-B)", Phys. Stat. Sol. 1978;49:387-392.
23. Ichikawa T. Electron Diffraction Study of the Local Atomic Arrangement in Amorphous Iron and Nickel Films. Phys. Stat. Sol. 1973;(a)19:707-716.